Antiviral Research 83 (2009) 103–111

Contents lists available at ScienceDirect

Antiviral Research

journal homepage: www.elsevier.com/locate/antiviral

In vitro and in vivo pharmacokinetic characterization of two novel prodrugs of zidovudine

Mario Alfredo Quevedo*, Margarita Cristina Briñón

Department of Pharmacy, Faculty of Chemical Sciences, National University of Córdoba, Haya de la Torre esq. Medina Allende s/n, Ciudad Universitaria, 5000 Córdoba, Argentina

ARTICLE INFO

Article history:
Received 2 January 2009
Received in revised form 18 March 2009
Accepted 27 March 2009

Keywords:
AZT prodrugs
Intestinal permeation
Plasma profiles
Plasma stability

ABSTRACT

This work deals with the in vitro and in vivo pharmacokinetic characterization of 3′-azido-2′,3′-dideoxy-5′-*O*-oxalatoylthymidine (AZT-Ac) and 3′-azido-2′,3′-dideoxy-5′-*O*-isonicotinoyl-thymidine (AZT-Iso), two novel prodrugs of the anti-HIV agent zidovudine [3′-azido-2′,3′-dideoxythymidine (AZT)]. AZT, AZT-Ac and AZT-Iso intestinal permeation properties and plasma concentration profiles in rats after intravenous administration were studied. Using the everted gut sac intestinal permeation assay, it was observed that AZT was subjected to saturable transport mechanisms in the jejunum and the proximal ileum, while no saturation was found in the distal ileum. AZT-Ac was able to permeate the intestinal segment at a lower rate than AZT but resisting enzymatic hydrolysis, while no evidence of saturation was found. On the other hand, AZT-Iso was completely hydrolyzed in the intestinal tissue, with AZT being found in the permeated samples. In vivo studies demonstrated that AZT plasma half-life ($t_{1/2}$) is extended after administration of AZT-Ac compared to AZT (2.16 and 0.96 h, respectively), while after administering AZT-Iso the $t_{1/2}$ of the regenerated AZT was shorter (0.38 h). A relationship is proposed between these observed in vivo pharmacokinetic features and previous studies of protein-binding properties, concluding that AZT-Ac is a very promising prodrug of AZT in the search for more effective and safer anti-HIV agents.

1. Introduction

Zidovudine (AZT, Fig. 1a) was the first drug approved by the Food and Drug Administration for the treatment of Acquired Immunodeficiency Syndrome (AIDS) in humans, and is still in use as part of the highly active antiretroviral therapy (HAART) regimen (De Clercq, 2009; Stürmer et al., 2007). Although its efficacy has long been demonstrated, some aspects such as cellular toxicity and suboptimal pharmacokinetic properties constitute a major concern (De Clercq, 2002). AZT cellular toxicity is manifested mainly by severe bone marrow aplasia, which leads to anemia and neutropenia (D'Andrea et al., 2008). It has been reported that these alterations originate mainly at the mitochondrial level, and include oxidative stress mechanisms and inhibition of the mitochondrial machinery (Scruggs and Dirks Naylor, 2008). Among its suboptimal pharmacokinetic aspects are its short plasma half-life ($t_{1/2} \approx 1$ h) (Barbier et al., 2000), low plasma protein-binding capacity (≈25% bound to total plasma proteins) (Luzier and Morse, 1993), and high hepatic glucuronidation rate (Moore et al., 1995). Another unfavorable pharmacokinetic issue is its incapacity to reach effective concentrations in viral reservoir tissues, such as the central nervous system (Pan et al., 2007; Eilers et al., 2008). As a consequence of these suboptimal properties of AZT, this drug needs to be administered frequently and in high doses, increasing the incidence of unwanted side effects, which usually compromises the adherence of the patient to the anti-HIV treatment. In this way, it has been accepted that there is still a need to improve several properties of this anti-HIV agent, mainly focusing in enhancing its oral bioavailability and prolonging its elimination half-life (De Clercq, 2007).

Several strategies have been applied in order to optimize the commented aspects, with the obtaining of prodrugs of AZT being a widely applied methodology (Calogeropoulou et al., 2003; Parang et al., 2000). In our research group we have synthesized several novel prodrugs of AZT, measuring their anti-HIV activity and cellular toxicity (Motura et al., 2002; Moroni et al., 2002; Turk et al., 2002). Within this family of compounds, two novel derivatives were of particular interest when considering their anti-HIV potency, cytotoxicity and physicochemical properties. These two compounds were obtained by functionalization of AZT leading to 3′-azido-3′-deoxy-5′-*O*-oxalatoylthymidine (AZT-Ac, Fig. 1b), and 3′-azido-3′-deoxy-5′-*O*-isonicotinoylthymidine (AZT-Iso, Fig. 1c) (Motura et al., 2002; Moroni et al., 2002).

Different studies have been performed as part of the preclinical development of these two novel prodrugs of AZT (Quevedo et

* Corresponding author. Tel.: +54 0351 4334163; fax: +54 0351 4334127.
E-mail address: alfredoq@fcq.unc.edu.ar (M.A. Quevedo).

0166-3542/$ – see front matter © 2009 Elsevier B.V. All rights reserved.
doi:10.1016/j.antiviral.2009.03.010

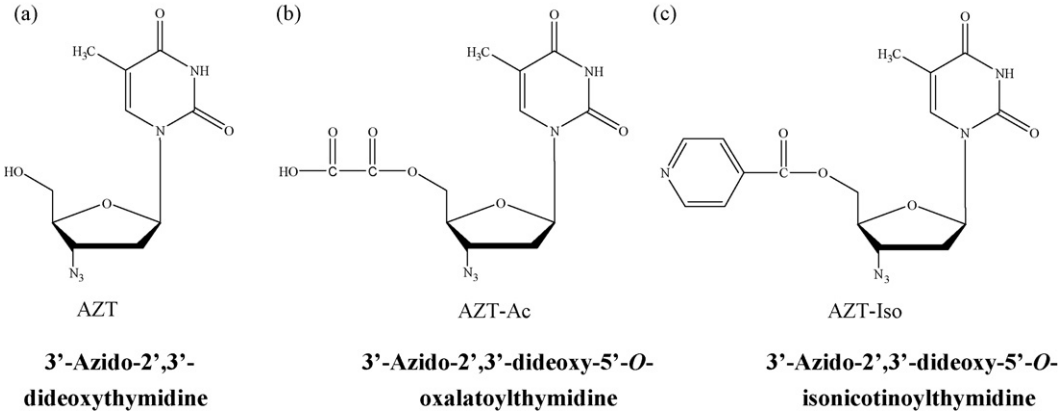

Fig. 1. Chemical structures of the compounds studied.

al., 2001, 2006; Teijeiro et al., 2003; Teijeiro and Briñón, 2006). In order to evaluate the benefits that the administration of AZT-Ac and AZT-Iso would represent with respect to AZT, and mainly referred to their oral bioavailability and capacity to prolong AZT elimination half-life, in this work we report intestinal permeation studies using rat intestinal segments and plasma concentration profiles after intravenous administration of AZT, AZT-Ac and AZT-Iso.

2. Materials and methods

2.1. Chemicals and reagents

AZT was kindly provided by Filaxis Laboratories (Buenos Aires, Argentina), while AZT-Ac and AZT-Iso were prepared as previously reported (Motura et al., 2002; Moroni et al., 2002). The Krebs buffer intended for intestinal permeation assays contained 119.0 mM NaCl, 4.7 mM KCl, 3.0 mM $CaCl_2$, 2.4 mM $MgSO_4$, 2.7 mM KH_2PO_4, 24.1 mM $NaHCO_3$ and 11 mM of glucose, while the modified Krebs buffer contained 119.0 mM NaCl, 4.7 mM KCl, 2.4 mM MgSO4, 2.7 mM KH_2PO_4, 24.1 mM $KHPO_4$ and 11 mM of glucose. All other chemicals and reagents used were of analytical grade. MilliQ grade water was used for the preparation of all solutions.

2.2. Apparatus

HPLC measurements were performed with three different sets of equipment depending on the analytical requirements. System A consisted of a Spectra System P2000 chromatograph, equipped with a Thermo Separation Products Spectra 100 UV variable wavelength detector set at 267 nm. Data acquisition was performed with the Peaksimple® v.2.86 software. System B consisted of an Agilent S1100 chromatograph, equipped with a multiple wavelength detector set at 267 nm, with data acquisition performed by the Chemstation Rev.A.10.02 package. System C was a Shimadzu LC-10ADvp chromatograph coupled to a Waters Quattro Micro triple quadrupole mass spectrometer, equipped with an API electron spray (ESI) interface and performing data acquisition with the MassLynx v.4.0 software. A Haake-DS thermostat bath (±0.1 °C) was used for assays requiring temperature control, while pH measurements were performed with a Crison GLP-21 pH meter.

2.3. Chemical stability

Solutions of AZT-Iso and AZT-Ac (50 ml, 270 μg/ml) were prepared in Krebs buffer (CO_2:O_2, 5%:95%), single Krebs buffer constituents and modified Krebs buffer (O_2, 100%), and incubated at 37 °C. Aliquots (2 ml) were sampled at suitable intervals, and subjected to the corresponding preparation and quantification procedure, obtaining plots of the remaining drug concentration vs. time. Linear regression analyses were performed (Microcal Origin v.7.0), calculating the observed hydrolysis constant (k_{obs}) and $t_{1/2}$.

2.4. Animal treatments

All procedures involving the use of rats were reviewed and approved by the Committee of Ethics for the Use of Animals in Experimental Protocols of the Faculty of Chemical Sciences, National University of Córdoba (FCS-UNC), Argentina (Res. No. 138/07). Adult male Wistar rats weighing 250–300 g were obtained from the bioterium of the Biological Chemistry Department, FCS-UNC, Argentina. Animals intended for intestinal permeation studies were fasted for 24 h prior to the assay, allowing free access to water. Animals used for the determination of plasma concentration profiles were caged with free access to food pellets and water until surgical procedures were performed.

2.5. Intestinal permeation assays

The intestinal permeation of AZT, AZT-Ac and AZT-Iso was studied applying the everted intestinal sac technique (Sharma et al., 2002). After rats were anesthetized by intraperitoneal administration of urethane (1000 mg/kg), a 2 cm incision was made in the midline abdominal cavity, isolating the segment of proximal jejunum (just 15 cm distal to the ligament of Treitz), followed by a second 15 cm segment of distal jejunum. In addition, two consecutive segments of 15 cm each were isolated immediately proximal to the cecum, and were named proximal and distal ileum, respectively. After the tissues were obtained, rats were sacrificed by an intracardiac bolus of urethane. The excised intestinal segments were immediately flushed with 80 ml of assay buffer solution to eliminate intestinal contents, and gently everted on a glass rod. During manipulation, segments were maintained submerged in the incubation media to assure tissue viability. A 10 cm glass cannula was inserted into the lumen (serosal side) of each everted segment, and tied at the top and end, placing a 10 g weight at the bottom of the segment (Fig. 2). The device containing the tissue was then submerged into 50 ml of solution containing the drug (mucosal solution) and thermostatized at 37 °C. 1 ml of buffer was placed through the glass cannula into the intestinal segment (serosal solution) and withdrawn at 15, 25, 35, 45, 55, 65, 75 and 85 min, applying 1 ml of fresh buffer to wash the glass cannula prior to the application of the next serosal solution sample. The collected aliquots were subjected to HPLC analyses after applying the corresponding preparation procedure. Permeation assays

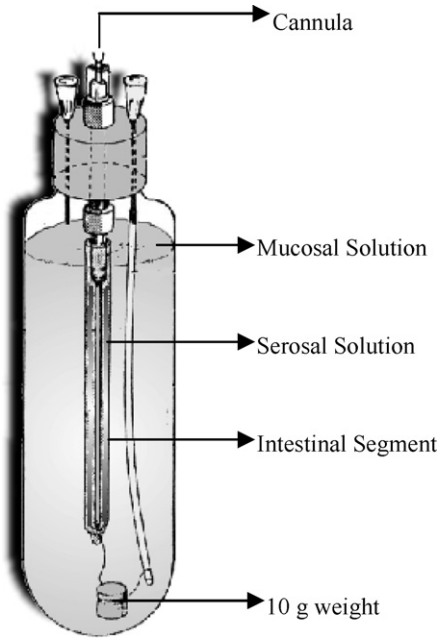

Fig. 2. Design of the device used for the everted gut sac intestinal permeation assay.

were performed in triplicate for each segment and concentration studied.

2.6. Sample preparation from intestinal permeation studies

2.6.1. AZT and AZT-Iso

A previously reported technique was applied (Quevedo et al., 2006). Briefly, Sep Pak Plus® (500 mg, Phenomenex®) C18 solid phase extraction (SPE) cartridges were preconditioned by the passage of 5 ml of HPLC-grade acetonitrile (ACN), followed by 5 ml of pH 2.6 sodium citrate buffer (0.1 M). 0.3 ml of internal standard solution containing *p*-fluorophenol (0.48 mg/ml) and 2.5 ml of pH 2.6 sodium citrate buffer (0.1 M) were added to the permeation samples, homogenized and applied to the preconditioned cartridge at a flow rate of 1 drop/s. The cartridge was dried, after which the drug was eluted with 5 ml of HPLC-grade ACN. The solution was filtered through 0.45 μm pore diameter membranes and subjected to HPLC analysis. Drug recoveries were adequate as reported previously (Quevedo et al., 2006).

2.6.2. AZT-Ac

Strata X® (60 mg, Phenomenex®) SPE cartridges were preconditioned by sequentially applying 1.5 ml of HPLC-grade ACN followed by 1.5 ml of pH 2.0 sodium phosphate buffer (0.1 M). Then 0.750 ml of pH 2.0 sodium phosphate buffer (0.1 M) were added to a 0.250 ml aliquot of the permeation sample, homogenized and applied to the preconditioned cartridge at a 1 drop/s flow rate. The extracted drug was eluted with 1.5 ml of an HPLC-grade ACN:pH 2.0 sodium phosphate buffer (0.1 M) 25:75 mixture. Drug recoveries were determined within the range of expected concentrations, finding quantitative and reproducible recoveries (Table 1).

2.7. HPLC and data analyses for intestinal permeation assays

2.7.1. AZT and AZT-Iso

Quantification was performed using System A described in the apparatus section. An Alltech Allsphere® C-18 (250 mm × 4.5 mm i.d.) column coupled to an AllGuard® C-18 guard column was used. The mobile phase consisted of a methanol:water (MeOH:H_2O, 60:40) mixture at a constant flow rate of 1 ml/min, injecting 20 μl of solution in each assay. Analytical parameters for the technique were previously validated (Quevedo et al., 2006).

Table 1
Recovery of AZT, AZT-Ac and AZT-Iso from different matrices, determined by solid phase extraction procedures.

Drug/matrix	Conc. (μg/ml)	Recovery (%)
AZT-Ac/mod. Krebs buff.	15	97.20 (±1.40)
	49	98.50 (±3.20)
AZT/rat plasma	0.15	95.13 (±3.12)
	3.00	94.70 (±4.05)
	6.00	97.22 (±2.70)
	14.4	97.88 (±2.05)
	49.0	98.50 (±1.27)
	101.8	97.18 (±3.91)
AZT-Ac/rat plasma	15	95.70 (±3.80)
	49	100.86 (±5.1)
AZT-Iso/rat plasma	0.15	98.70 (±17.08)
	3.00	96.65 (±3.68)
	6.00	81.47 (±2.70)

2.7.2. AZT-Ac

Quantification was performed using System B described in the apparatus section. A Phenomenex Synergy Fusion® C-18 (250 mm × 4 mm i.d.) column and a Phenomenex Security Guard Fusion® RP (4 mm × 30 mm) guard column were used. The mobile phase consisted of a pH 2.0 sodium phosphate buffer (0.025 M):MeOH:tetrahydrofuran (THF) (68:30:2) mixture, at a constant flow rate of 1 ml/min. Analyses were performed at 40 °C, injecting 100 μl of solution in each assay. The corresponding calibration curves were constructed, finding linear responses in the range 0.2–6.0 μg/ml. The lowest limit of detection (LLOD) and lowest limit of quantitation (LLOQ) were 0.09 and 0.28 μg/ml, respectively. Adequate intraday/interday accuracy and precisions were obtained.

2.7.3. Data analysis

The amount of drug accumulated in the serosal solution (μg) vs. time (min) was plotted. After performing a linear regression analysis, the flux (*F*, μg/min) was obtained from the slope and the apparent permeability coefficient (P_{app}) was calculated applying Eqs. (1) and (2) (Sharma et al., 2002):

$$P_{app} = \frac{F}{\mathrm{Sup}_{exp} \cdot C_i} \quad (1)$$

$$\mathrm{Sup}_{exp} = 2\pi rh \quad (2)$$

were Sup_{exp} is the surface available for permeation, C_i is the initial concentration of drug in the mucosal solution, *r* is the intestinal segment mean radii (0.4 cm) and h is the length of intestinal segment available for permeation (10 cm).

2.8. Plasma concentration profiles

Rats were anesthetized with urethane (1000 mg/kg, i.p.) and the right femoral vein and left femoral artery were cannulated with heparinized PE-10 (Becton, Dickinson and Company®) catheters (Waynforth and Flecknell, 1992). Drug solutions (20 mg/kg for AZT and AZT-Ac, and 2.5 mg/kg for AZT-Iso) were administered through the right femoral vein as a single intravenous bolus (0.3 ml/min) dissolved in sterile normal saline solution containing 10% of dimethylsulfoxide (DMSO). After administering the bolus, the cannula was rinsed with 0.1 ml of heparinized saline solution. Blood samples were collected from the left femoral artery, and to assure sampling of central fluids, the following protocol was applied: 0.3 ml of blood were withdrawn in a first step, after which 0.15 ml were collected for quantitation purposes, while the 0.3 ml of blood collected in the first step were reinfused to the animal via

the femoral vein; 0.15 ml of heparinized saline solution was used to flush the cannula and replace the sample volume. Blood was immediately centrifuged at 2000 rpm, collecting 50 μl of plasma, which was subjected to the corresponding preparation procedure.

2.9. Rat plasma sample preparation

Samples of 50 μl of plasma were diluted to 1 ml with pH 2.0 sodium phosphate buffer (0.05 M) for AZT and AZT-Ac, while pH 2.6 sodium citrate buffer (0.05 M) was used as dilution solvent for AZT-Iso. The resulting solutions were applied to Strata X (60 mg, Phenomenex®) SPE cartridges, which were previously preconditioned with 1 ml of HPLC-grade ACN and 1 ml of the corresponding dilution solvent. The resulting solutions were applied to the cartridge at a flow rate of 1 drop/s, after which it was washed with 0.5 ml of fresh dilution solvent and dried. Finally, the elution of the drug was performed with 1.5 ml of ACN:sodium phosphate pH 2.0 buffer (0.05 M) (25:75) mixture for AZT and AZT-Ac and ACN:H_2O (25:75) for AZT-Iso, filtered through 0.45 μm pore diameter membranes and subjected to HPLC analysis. Drug recovery assays from rat plasma were performed in the range of expected concentrations, finding quantitative and reproducible recoveries in the concentration range assayed (Table 1).

2.10. HPLC analysis of rat plasma samples

For the quantification of AZT and AZT-Ac, identical methodology used for the intestinal permeation assays was applied (see Section 2.7). For AZT-Iso and the corresponding regenerated AZT, System C described in the apparatus section was used, equipped with a Water Symmetry® C-18 (75 mm × 4.6 mm i.d.) column coupled to a Phenomenex Security Guard Fusion® RP (4 mm × 30 mm) guard column. The mobile phase consisted of a pH 5.0 ammonium acetate buffer (0.001 M):ACN (70:30) mixture, at a flow rate of 0.2 ml/min. Positive electron spray ionization mode was used, with single ion monitoring at *m/z* 268 and 373 for AZT and AZT-Iso, respectively. Maximum sensitivity of the system was achieved at the following instrument settings: heated capillary temperature: 120 °C, spray voltage: 2.90 kV, scan time: 1 s, collision cell voltage: 50 kV, electron multiplier voltage 650 V and desolvation gas (N_2) flow: 600 l/h.

3. Results

3.1. Chemical stability of AZT-Iso and AZT-Ac

In order to perform intestinal permeation assays, the chemical stability of the prodrugs in the mucosal solution needed to be studied. In this way, the k_{obs} found for AZT-Iso in pH 7.4 Krebs buffer (CO_2:O_2, 5:95%) was 0.015 min^{-1}, with a $t_{1/2}$ of 45.89 min. Considering that the drug needs to be stable during the assay (85 min), the $t_{1/2}$ found is quite short and thus high quantities of AZT would be regenerated due to chemical hydrolysis. Considering this, stability assays were performed in each constituent of the buffer, finding that AZT-Iso was highly unstable in sodium bicarbonate solutions. This fact was not due to the pH of the bicarbonate solution since, when Krebs buffer was adjusted to pH 7.4, a short $t_{1/2}$ was also observed, concluding that the presence of bicarbonate ions was able to catalyze the hydrolysis of AZT-Iso to AZT. Thus, the Krebs buffer was modified in a similar way to that previously reported (Kerr and Ong, 1987), replacing bicarbonate by a KH_2PO_4/$KHPO_4$ buffer. Also, $CaCl_2$ was removed due to precipitation of $Ca_3(PO_4)_2$. The final buffer solution was adjusted to pH 7.4 and gassed with 100% oxygen. When AZT-Iso chemical stability in this modified Krebs buffer was assayed, the k_{obs} was 9.70×10^{-4} min^{-1} with a $t_{1/2}$ of 714 min (12 h), which was now adequate. The stability of AZT-Ac in the modified Krebs buffer was also studied, finding no hydrolysis of the prodrug after 2 h of incubation at 37 °C. Considering these aspects, the modified Krebs buffer was selected to perform the intestinal permeation assays of AZT and these two prodrugs.

Considering that these prodrugs will transit along the gastrointestinal tract before absorption takes place, chemical stability in the pH range 1–7.4 was studied as part of their preformulation development. Our unpublished data indicated that AZT-Iso exhibited a marked increase in its stability as solution acidity increased, with $t_{1/2}$ ranging from 14.9 h at pH 7.4 to 346.5 h at pH 1. AZT-Ac chemical stability was not markedly influenced by the pH of the solution, with $t_{1/2}$ ranging from 17.3 h at pH 7.4 to 13.9 h at pH 1 (Briñón et al., unpublished data). Within the scope of this work, and considering that observed $t_{1/2}$ were high compared to the expected transit times from stomach to the ileocecal valve (≅3 h), it can be pointed out that both of these prodrugs exhibited an adequate chemical stability profile in the pH range of the gastrointestinal tract.

3.2. Intestinal permeation of AZT, AZT-Iso and AZT-Ac

The intestinal permeation of the studied compounds was evaluated employing the everted intestinal sac technique (Sharma et al., 2002). Considering that the permeation pattern of drugs may vary throughout the length of the small intestine, we analyzed AZT permeation through the proximal and distal jejunum, as well as in the proximal and distal ileum. Also, the concentration dependence was analyzed using mucosal solutions of 120, 200, 270, 570 and 1120 μg/ml of AZT. As an example, Fig. 3 shows the plots corresponding to the amount of AZT accumulated in the serosal solution

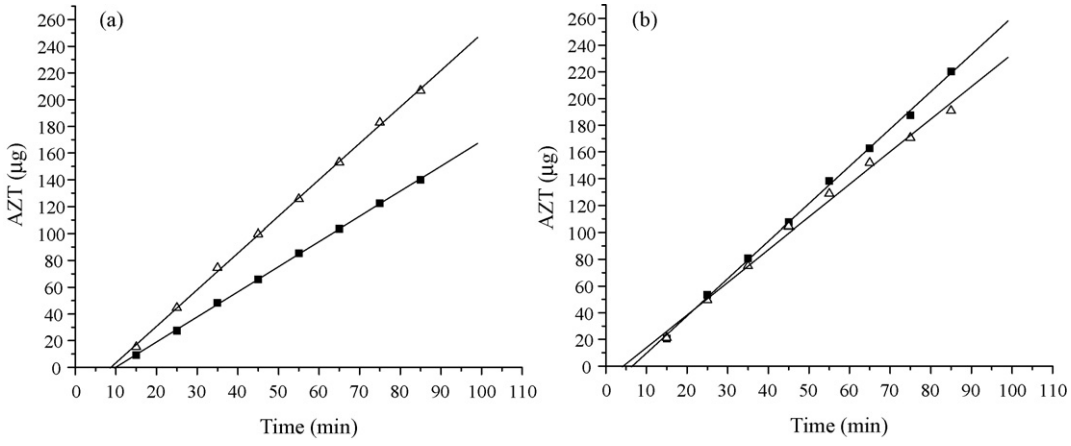

Fig. 3. Plots of the amount of AZT accumulated vs. time in the mucosal solution of: (a) proximal (■) and distal jejunum (△); (b) proximal (■) and distal ileum (△).

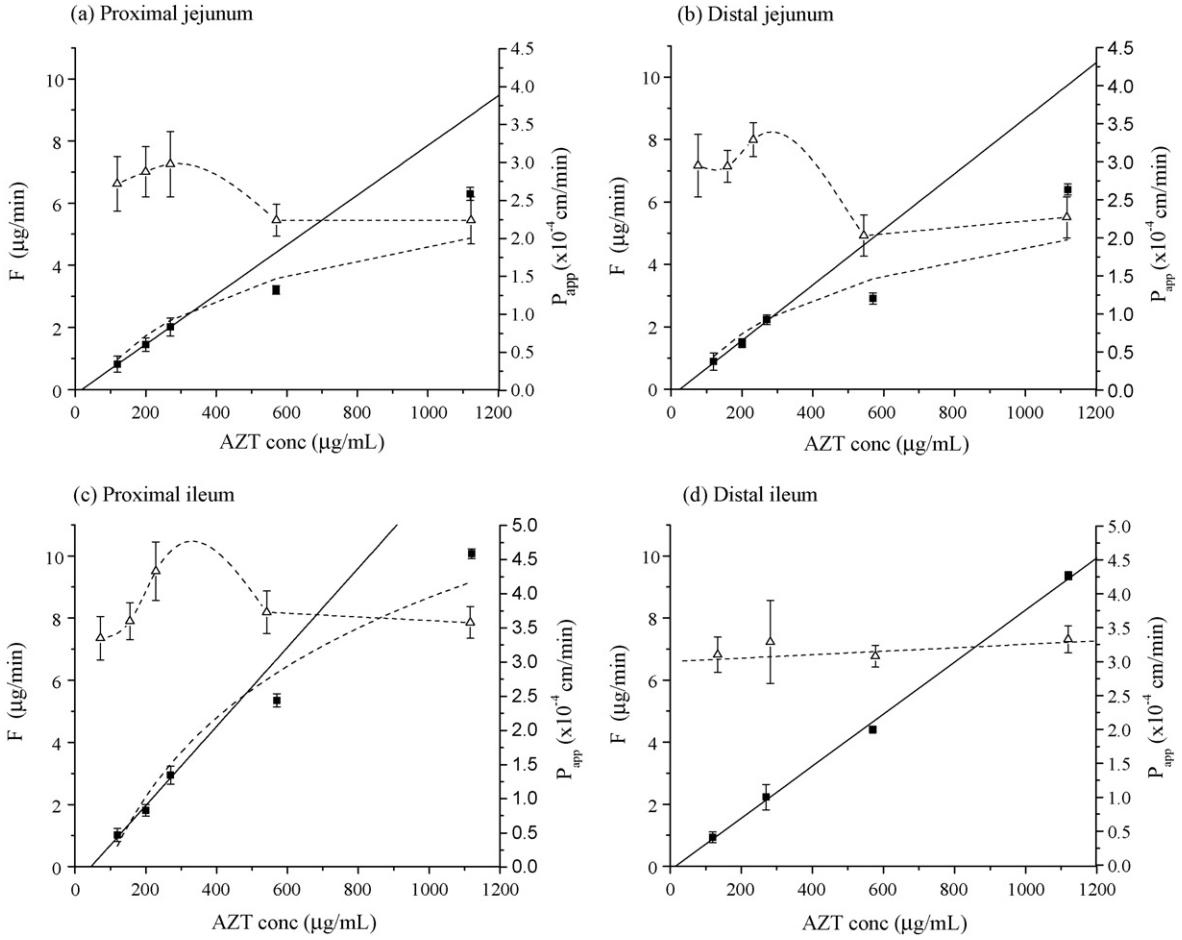

Fig. 4. Plots of the flux (F, ■) vs. concentration and intestinal permeability coefficient (P_{app}, △) vs. concentration for the permeation of AZT through: (a) proximal jejunum, (b) distal jejunum, (c) proximal ileum and (d) distal ileum.

vs. time at 270 μg/ml for the four intestinal segments. The corresponding linear regression equations (Eqs. (3)–(6)) were obtained, from which the flux (F) and apparent permeability coefficient (P_{app}) values were calculated using Eqs. (1) and (2).

Proximal jejunum

$$\mu g\ AZT = 1.88\ (\pm 0.01)\ Time - 18.55\ (\pm 0.69) \quad (3)$$
$$r = 0.9999;\ R^2 = 0.9992;\ sd = 0.81;\ n = 8;\ F = 22384.51$$

Distal jejunum

$$\mu g\ AZT = 2.32\ (\pm 0.03)\ Time - 23.86\ (\pm 1.44) \quad (4)$$
$$r = 0.9997;\ R^2 = 0.9991;\ sd = 1.69;\ n = 8;\ F = 10888.26$$

Proximal ileum

$$\mu g\ AZT = 2.79\ (\pm 0.04)\ Time - 18.14\ (\pm 2.21) \quad (5)$$
$$r = 0.9994;\ R^2 = 0.9987;\ sd = 2.60;\ n = 8;\ F = 4829.30$$

Distal ileum

$$\mu g\ AZT = 2.44\ (\pm 0.07)\ Time - 10.44\ (\pm 4.01) \quad (6)$$
$$r = 0.9973;\ R^2 = 0.9868;\ sd = 4.72;\ n = 8;\ F = 1118.83$$

Values of F and P_{app} for all the concentrations and intestinal segments were evaluated, from which the relationship with drug concentration was analyzed (Fig. 4).

When the permeation of AZT-Iso was assayed at 270 μg/ml in distal jejunum, only AZT was detected in the serosal solution, indicating that the prodrug was completely hydrolyzed during its passage through the intestinal segment. The F and P_{app} for the regenerated AZT were 2.36 (±0.17) μg/min and 3.46 (±0.26) $\times 10^{-4}$ cm/min, respectively, which were not significantly different from those obtained from mucosal solutions containing AZT [2.23 (±0.15) and 3.29 (±0.22) $\times 10^{-4}$ cm/min, respectively].

The permeation of AZT-Ac was initially studied at 270 μg/ml in the distal jejunum; intact prodrug was found in the serosal solution, but no AZT at all was found. Considering the fact that the prodrug was able to resist hydrolysis during its permeation process, the F and P_{app} were found between 200 and 1000 μg/ml (Fig. 5).

3.3. Stability of the prodrugs in rat plasma

The stability of AZT-Iso was determined in our previous work (Quevedo et al., 2006), this prodrug is moderately stable in rat plasma with a $t_{1/2}$ of 1.12 h. The stability of AZT-Ac in rat plasma was assayed before determining its plasma profiles, observing that its hydrolysis was rapid, and that after 20 min of incubation at 37 °C almost all the prodrug was hydrolyzed to AZT.

3.4. Plasma profiles of AZT, AZT-Ac and AZT-Iso

The plasma concentration vs. time profile of AZT (20 mg/kg) was obtained (Fig. 6a), performing the corresponding compartmental analyses to adjust AZT plasma concentrations to a one- and two-compartment models. From the statistical analyses, which included comparison of mean standard errors (MSE), coefficients of determination (R^2) and the Akaike test (Bonate, 2006), it was concluded that AZT is better fitted to a one-compartment model. Pharmacokinetic parameters were calculated using the PK Solutions 2.0 software, finding a $t_{1/2}$ of 0.96 (±0.05) h, a volume of distribution (V_d) of

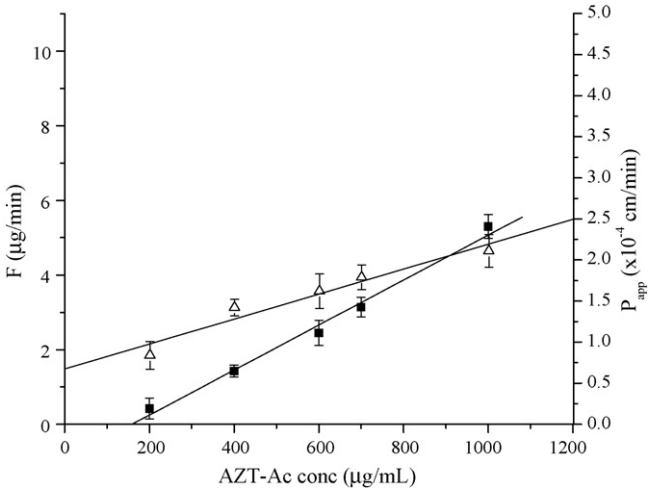

Fig. 5. Plots of the flux (F, ■) vs. concentration and intestinal permeability coefficient (P_{app}, △) vs. concentration for the permeation of AZT-Ac through distal jejunum.

0.724 (±0.09) l/kg and a plasma clearance (Cl_p) of 0.533 (±0.060) l/h kg.

In a similar way, the plasma vs. time concentration profile of AZT-Ac (20 mg/kg) was obtained. After performing the quantification, only the presence of AZT was detected in plasma, demonstrating that the prodrug is rapidly hydrolyzed in vivo, an observation that is consistent with the in vitro plasma stability studies. The concentration vs. time profile of the AZT regenerated from AZT-Ac was analyzed, a finding that was best fitted by a two-compartment model, with a rapid initial distribution phase, followed by a slower elimination phase. In order to be able to describe better the initial distribution phase, the sampling protocol included three additional data points at 5, 15 and 70 min (Fig. 6a). After performing the corresponding mathematical analyses, the following pharmacokinetic parameters were calculated: (a) $t_{1/2}$ distribution phase: 0.03 (±0.01) h, (b) $t_{1/2}$ elimination phase: 2.16 (±0.35) h, (c) V_d: 0.762 (±0.068) l/kg and (d) Cl_p: 0.246 l/h kg.

In order to study the in vivo pharmacokinetic properties of AZT-Iso, it was not possible to administer a 20 mg/kg dose of prodrug due to solubility problems in the vehicle. This problem could not be overcome by increasing the amount of cosolvent, since adequate solubilization of the prodrug was achieved only at 50% (v/v) of DMSO, but a concomitant hemolysis was observed when this solution was administered to the rat. Also, the problem could not be solved using other cosolvents such as Tween® 80 or ethanol. In this way, the minimum dose of prodrug compatible with solubilization in 0.3 ml of vehicle was 2.5 mg/kg, thus this dose of drug was administered to the rat. After quantification, both AZT and AZT-Iso were found in plasma, with concentrations of AZT declining rapidly between 0 and 40 min (Fig. 6b), describing a one-compartment model with the following associated pharmacokinetic parameters: $t_{1/2}$ 0.38 (±0.05) h, V_d 0.917 (±0.060) l/kg and Cl_p 1.67 (±0.118) l/h kg. Plasma concentrations of the intact prodrug were considerably lower than those of AZT (Fig. 6b), and a high variability was observed in their concentration, which may be due to the high variability in its recovery by SPE at low concentrations (Table 1).

4. Discussion

4.1. Intestinal permeation of AZT, AZT-Iso and AZT-Ac

When analyzing the intestinal permeation properties of AZT in proximal jejunum (Fig. 4a), a linear increase in F was found between 120 and 270 µg/ml, with a deviation from linearity at higher concentrations (570 and 1120 µg/ml). Also, ANOVA analyses indicated that the P_{app} at 570 and 1120 µg/ml are reduced compared to lower concentrations, suggesting that a saturable transport mechanism is involved in AZT permeation through the proximal jejunum. For the distal jejunum (Fig. 4b) a similar pattern was observed, with a linear relationship between the concentration and F in the range 120–270 µg/ml, and a deviation from this linearity at higher concentrations. The P_{app} values between 120 and 270 µg/ml were statistically equivalent, while at the two higher concentrations lower values were confirmed by the ANOVA test, suggesting that the transport of AZT in this segment also involves a saturable mechanism.

When AZT permeation was studied in the proximal ileum (Fig. 4c), the linearity between the concentration and F in the 120–270 µg/ml range was still observed, finding again deviation from linearity at the two higher concentrations. Also, higher P_{app} values were found with the increase of the concentration between 120 and 270 µg/ml, suggesting that a transport mechanism that increases its capacity with the increase of drug concentration is involved. In the distal ileum segment (Fig. 4d), no deviation from linearity was observed when plotting F vs. concentration, and the P_{app} was also found to be constant in the range of concentrations assayed. This observation suggests two alternatives: (a) the involvement of a non-saturable transport, or (b) a transport mechanism with higher capacity than that of the previous intestinal segments, exhibiting no saturation at the concentrations assayed. Comparing

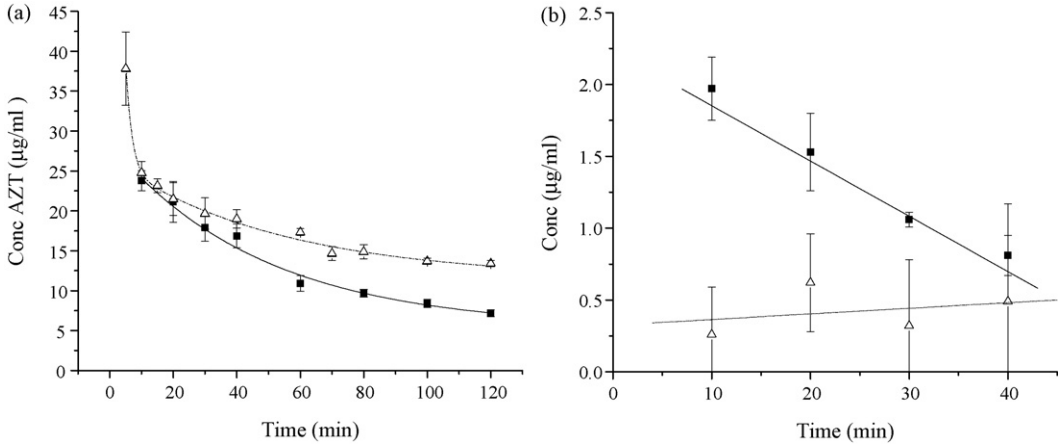

Fig. 6. (a) Plasma concentration profile of AZT determined in rats after intravenous administration of AZT (20 mg/kg, ■) and AZT-Ac (20 mg/kg, △). (b) Plasma concentration profile of AZT (■) and AZT-Iso (△) determined in rats after intravenous administration of AZT-Iso (2.5 mg/kg).

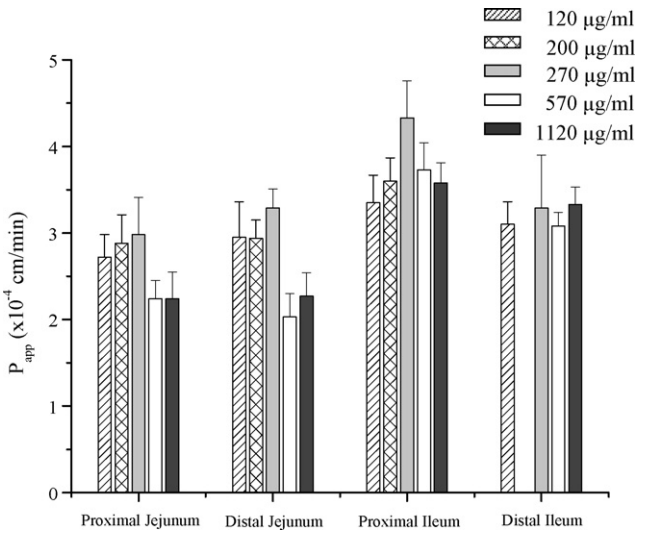

Fig. 7. Intestinal permeability coefficients (P_{app}) of AZT determined at various drug concentrations and in different intestinal segments.

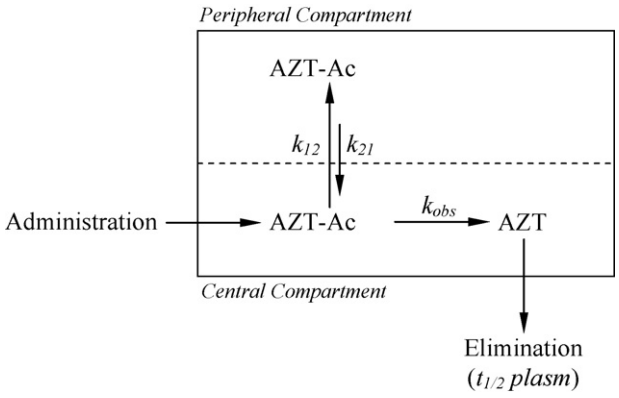

Fig. 8. Distribution model of AZT-Ac between the peripheral and central compartment as concluded from the two-compartmental models observed.

the segments all together (Fig. 7), P_{app} values in both regions of the jejunum were statistically equivalent, exhibiting a similar transport saturation pattern, while the permeation through proximal ileum was considerably enhanced compared to the jejunum segments.

This observation, summed to the lack of saturation in the distal ileum, suggest that specific transporters of AZT may increase their tissue expression towards the distal portions of small intestine. It has been previously proposed that sodium-dependent nucleoside transporters are involved in the transport of AZT in small intestine (Balimane and Sinko, 1999), and considering that these transporters are mainly expressed in the proximal segments of small intestine (Huang et al., 1993), it is possible that the permeation pattern observed in the jejunum segments is originated by the saturation of these transporters. Clearly, the transport of AZT in the ileum involves a different kind of transporter than in jejunum.

Taking into account that both AZT-Iso and AZT-Ac were designed as prodrugs of AZT with the aim to obtain anti-HIV agents with higher bioavailability, it was of particular interest to analyze if these two novel compounds were subjected to the same transport mechanism(s) as AZT. In this way, the distal jejunum segment was selected as a model to study their permeation properties.

Regarding the intestinal permeation properties of AZT-Iso, we observed that it was completely hydrolyzed when crossing the intestinal tissue, a fact that constitutes a serious limitation for its development as a prodrug intended for oral administration. Considering that the lipophilicity of AZT-Iso is significantly increased with respect to that of AZT (Teijeiro et al., 2000), we should have expected that passive diffusion by contributing to the intestinal permeation would have enhanced its ability to cross the intestinal tissue. It is possible that the transcellular passage of the prodrug through the enterocyte makes the prodrug to get in contact with intestinal esterases, and thus the prodrug is efficiently hydrolyzed. Considering the commented results, the applicability of AZT-Iso would be limited to an intravenous administration route.

When analyzing AZT-Ac intestinal permeation (Fig. 5), a linear relationship between F and the concentration was found. Also, ANOVA analyses on the P_{app} at different concentrations showed an increase of the permeability with an increase of drug concentration, indicating an enhancement of the transport capacity of this prodrug at higher concentrations. This observation suggests two possibilities: (a) the involvement of a transport mechanism which increase its capacity at higher drug concentrations, and/or (b) the saturation of efflux transporters (Szakács et al., 2008), causing higher concentrations of drug in the serosal side and the corresponding increase in the P_{app}. Considering that it has been recently reported that active efflux mechanisms of AZT are present not only at the intestinal level, but also in other tissues (Pan et al., 2007; Eilers et al., 2008), the features observed for the intestinal permeation of AZT-Ac are of particular interest in the context of the pharmacokinetic properties of this prodrug. It needs to be pointed out that the P_{app} values found for AZT-Ac at low concentrations are considerably lower than those of AZT, a fact that would generate a lower bioavailability of the prodrug with respect to that of the leader compound, but also as a consequence of the increase in P_{app} at higher concentrations, the permeability at high concentrations for both compounds being comparable. Although further studies regarding the specific mechanism involved during its intestinal permeation are required, it is clear that AZT-Ac may be useful as a prodrug for oral administration.

4.2. Plasma profiles of AZT, AZT-Ac and AZT-Iso

The one-compartment model observed for the plasmatic profile of AZT is in agreement with previous work using slightly different experimental designs (Song et al., 2002; Brown et al., 2003; Wientjes and Au, 1992), in which similar $t_{1/2}$ were reported. This observation indicates that the experimental procedures applied are adequate to study the in vivo pharmacokinetic properties of AZT and its prodrugs.

The one- and two-compartment models found after administration of AZT and AZT-Ac, respectively, suggest differences in the tissue distribution of these two compounds, evidencing a higher affinity of the prodrug for peripheral tissues compared to AZT. The microconstants k_{12} and k_{21} (Fig. 8) determine the speed at which the prodrug equilibrates between the peripheral and the central compartment. These magnitudes were calculated from the equation defining the two-compartment model (Welling, 1997), finding values of 0.265 and 0.079 min^{-1} for k_{12} and k_{21}, respectively.

These values indicates that AZT-Ac exhibits a 3.4-fold higher affinity for the peripheral compartment than for the central one, typically represented by the intravascular fluid and highly perfused tissues, while the peripheral compartment is usually defining poorly perfused organs. Since the perfusion pattern is homologous when comparing the administration of AZT and AZT-Ac, differential affinities of these compounds for constituents of both compartments may be involved in defining the observed phenomena. In a previous work (Quevedo et al., 2008), a detailed study of the affinity of AZT-Ac to human serum albumin (HSA) was performed, suggesting that the presence of HSA in intravascular and extravascular fluids, may lead to differences of AZT and its prodrugs in tissue affinities. In this way, HSA present in the intravascular fluids is complexed with fatty acids (HSA_{FA}), phenomena that diminish

AZT-Ac affinity for the macromolecule (Quevedo et al., 2008). On the other hand, and considering the low content of free fatty acids in extravascular fluids (Parini et al., 2006), HSA is expected to be in its pure state (HSA_P) in the peripheral compartment. As has been previously reported, AZT-Ac exhibits a low bound fraction to HSA_{FA} (10.4%) due to an electrostatic repulsion phenomenon with a fatty acid moiety bound to Sudlow site I, while the bound fraction is considerably increased for HSA_P (47%) due to the establishment of ionic interactions with aminoacid side chains located in the binding site cavity. In this way, AZT-Ac would exhibit a higher affinity for extravascular fluids than for intravascular ones, giving rise to the observed two-compartment model. Considering that elimination of AZT is mainly due to glucuronidation of the drug present in the blood (Barbier et al., 2000), the higher affinity for extravascular components would also be responsible for the prolonged $t_{1/2}$ of AZT after administration of AZT-Ac (2.16 ± 0.05 h). Analyzing AZT protein-binding properties, we have reported a higher affinity for HSA_{FA} than for HSA_P (Quevedo et al., 2008), and thus this drug would accumulate in the intravascular fluids, which is in agreement with the one-compartment model and the shorter $t_{1/2}$ found (0.95 ± 0.05 h). Analyzing AZT-Iso HSA binding properties (Quevedo et al., 2008) and its plasmatic concentration profiles, we observe that this prodrug exhibits a higher bound fraction to HSA_{FA} than AZT (38.8% and 21.2%, respectively), which would give a higher affinity for the intravascular compartment and the consequently lower $t_{1/2}$ for the AZT regenerated in vivo. This is explaining the short $t_{1/2}$ found for AZT after administration of AZT-Iso (0.38 h) compared to AZT or AZT-Ac (0.95 and 2.16 h, respectively). These results suggest that the design of prodrugs of AZT based on selective affinity for HSA_{FA} and HSA_P may be a very interesting strategy not only to prolong AZT elimination half-life, but also to target this antiviral agent to extravascular tissues such as the lymphatic system. This would provide an enhanced potency and also lower risk of potential side effects. The use of modified HSA targeted to viral reservoirs, such as the lymphatic system, has also been previously considered (Swart et al., 1999).

Based on this work, we can conclude that continuing the development of AZT-Ac as a new anti-HIV agent would be very promising, since it not only demonstrated interesting intestinal permeation features, but also showed the capacity to increase AZT $t_{1/2}$ in vivo. These properties, added to its promising antiviral activity and lower cytotoxicity (Turk et al., 2002), makes this prodrug a very interesting compound in the search for more effective and safer anti-HIV drugs. Finally, obtaining AZT prodrugs based on a selective binding affinity for HSA_{FA} and HSA_P is also seen as an interesting strategy that merits deeper investigation.

Acknowledgements

The authors gratefully acknowledge financial support from the Secretaria de Ciencia y Técnica of the Universidad Nacional de Córdoba (SECYT-UNC), the Consejo Nacional de Investigaciones Científicas y Técnicas (CONICET) and the Agencia Nacional de Promoción Científica y Tecnológica (FONCyT) of Argentina. The authors would also like to thank Dr. L. Alassia (FILAXIS Laboratories) for supplying AZT, and Dr. Anselmo Gomes de Oliveira and Dra. Rosângela Gonçalves Peccinini Machado, Faculty of Pharmaceutical Sciences, UNESP, Araraquara, Brasil, for enabling HPLC-MS/MS analyses. Mario A. Quevedo also acknowledges the receipt of fellowships from CONICET.

References

Balimane, P.V., Sinko, P.J., 1999. Involvement of multiple transporters in the oral absorption of nucleoside analogues. Adv. Drug Deliv. Rev. 39, 183–209.

Barbier, O., Turgeon, D., Girard, C., Green, M.D., Tephly, T.R., Hum, D.W., Bélanger, A., 2000. 3′-Azido-3′-deoxythymidine (AZT) is glucuronidated by human UDP-glucuronosyltransferase 2B7 (UGT2B7). Drug Metab. Dispos. 28, 497–502.

Bonate, P.L., 2006. The art of modeling. In: Pharmacokinetic–Pharmacodynamic Modeling and Simulation. Springer, New York, pp. 1–56.

Brown, S.D., Bartlett, M.G., White, C.A., 2003. Pharmacokinetics of intravenous acyclovir, zidovudine, and acyclovir–zidovudine in pregnant rats. Antimicrob. Agents Chemother. 47, 991–996.

Calogeropoulou, T., Detsi, A., Lekkas, E., Koufaki, M., 2003. Strategies in the design of prodrugs of anti-HIV agents. Curr. Top. Med. Chem. 3, 1467–1495.

D'Andrea, G., Brisdelli, F., Bozzi, A., 2008. AZT: an old drug with new perspectives. Curr. Clin. Pharmacol. 3, 20–37.

De Clercq, E., 2002. Molecular targets and compounds for anti HIV therapy. In: Matsoukas, J., Mavromoustakos, T. (Eds.), Drug Discovery and Design: Medical Aspects. IOS Press, Amsterdam, The Netherlands, pp. 272–278.

De Clercq, E., 2007. The design of drugs for HIV and HCV. Nat. Rev. Drug. Discov. 6, 1001–1018.

De Clercq, E., 2009. Anti-HIV drugs: 25 compounds approved within 25 years after the discovery of HIV. Int. J. Antimicrob. Agents 33, 307–320.

Eilers, M., Roy, U., Mondal, D., 2008. MRP (ABCC) transporters-mediated efflux of anti-HIV drugs, saquinavir and zidovudine, from human endothelial cells. Exp. Biol. Med. 233, 1149–1160.

Huang, Q.Q., Harvey, C.M., Paterson, A.R.P., Cass, C.E., Young, J.D., 1993. Functional expression of Na(+)-dependent nucleoside transport systems of rat intestine in isolated oocytes of *Xenopus laevis*. Demonstration that rat jejunum expresses the purine-selective system N1 (cif) and a second, novel system N3 having broad specificity for purine and pyrimidine nucleosides. J. Biol. Chem. 268, 20613–20619.

Kerr, D.I., Ong, J., 1987. Bicarbonate-dependence of responses to ethylenediamine in the guinea-pig isolated ileum: involvement of ethylenediamine-monocarbamate. Br. J. Pharmacol. 90, 763–769.

Luzier, A., Morse, G.D., 1993. Intravascular distribution of zidovudine: role of plasma proteins and whole blood components. Antiviral Res. 21, 267–280.

Moore, K.H., Raasch, R.H., Brouwer, K.L.R., Opheim, K., Cheeseman, S.H., Eyster, E., Lemon, S.M., van der Horst, C.M., 1995. Pharmacokinetics and bioavailability of zidovudine and its glucuronidated metabolite in patients with human immunodeficiency virus infection and hepatic disease (AIDS Clinical Trials Group protocol 062). Antimicrob. Agents Chemother. 39, 2732–2737.

Moroni, G.N., Bogdanov, P.M., Briñón, M.C., 2002. Synthesis and in vitro antibacterial activity of novel 5′-*O*-analog derivatives of zidovudine as potential prodrugs. Nucleosides Nucleotides Nucleic Acids 21, 231–241.

Motura, M.I., Moroni, G.N., Teijeiro, S.A., Salomón, H., Briñón, M.C., 2002. 3′-Azido-3′-deoxy-5′-*O*-isonicotinoylthymidine, a new prodrug of zidovudine. Synthesis, solid state characterization, and anti HIV-1 activity. Nucleosides Nucleotides Nucleic Acids 21, 217–230.

Pan, G., Giri, N., Elmquist, W.F., 2007. Abcg2/Bcrp1 mediates the polarized transport of antiretroviral nucleosides abacavir and zidovudine. Drug Metab. Dispos. 35, 1165–1173.

Parang, K., Wiebe, L.I., Knaus, E.E., 2000. Novel approaches for designing 5′-*O*-ester prodrugs of 3′-azido-2′, 3′-dideoxythymidine (AZT). Curr. Med. Chem. 7, 995–1039.

Parini, P., Johansson, L., Bröijersén, A., Angelin, B., Rudling, M., 2006. Lipoprotein profiles in plasma and interstitial fluid analyzed with an automated gel-filtration system. Eur. J. Clin. Invest. 36, 98–104.

Quevedo, M.A., Moroni, G.N., Briñoïn, M.C., 2001. Human serum albumin binding of novel antiretroviral nucleoside derivatives of AZT. Biochem. Biophys. Res. Commun. 288, 954–960.

Quevedo, M.A., Teijeiro, S.A., Briñón, M.C., 2006. Quantitative plasma determination of a novel antiretroviral derivative of zidovudine by solid-phase extraction and high-performance liquid chromatography. Anal. Bioanal. Chem. 385, 377–384.

Quevedo, M.A., Ribone, S.R., Moroni, G.N., Briñón, M.C., 2008. Binding to human serum albumin of zidovudine (AZT) and novel AZT derivatives. Experimental and theoretical analyses. Bioorg. Med. Chem. 16, 2779–2790.

Scruggs, E.R., Dirks Naylor, A.J., 2008. Mechanisms of zidovudine-induced mitochondrial toxicity and myopathy. Pharmacology 82, 83–88.

Sharma, P., Chawla, H.P., Panchagnula, R., 2002. LC determination of cephalosporins in in vitro rat intestinal sac absorption model. J. Pharm. Biomed. Anal. 27, 39–50.

Song, H., Griesgraber, G.W., Wagner, C.R., Zimmerman, C.L., 2002. Pharmacokinetics of amino acid phosphoramidate monoesters of zidovudine in rats. Antimicrob. Agents Chemother. 46, 1357–1363.

Stürmer, M., Staszewski, S., Doerr, H.W., 2007. Quadruple nucleoside therapy with zidovudine, lamivudine, abacavir and tenofovir in the treatment of HIV. Antivir. Ther. 12, 695–703.

Swart, P.J., Beljaars, L., Kuipers, M.E., Smit, C., Nieuwenhuis, P., Meijer, D.K., 1999. Homing of negatively charged albumins to the lymphatic system: general implications for drug targeting to peripheral tissues and viral reservoirs. Biochem. Pharmacol. 58, 1425–1435.

Szakács, G., Váradi, A., Ozvegy-Laczka, C., Sarkadi, B., 2008. The role of ABC transporters in drug absorption, distribution, metabolism, excretion and toxicity (ADME-Tox). Drug Discov. Today 13, 379–393.

Teijeiro, S.A., Moroni, G.N., Motura, M.I., Briñón, M.C., 2000. Lipophilic character of pyrimidinic nucleoside derivatives: correlation between shake flask, chromato-

graphic (RP-TLC and RP-HPLC) and theoretical methods. J. Liq. Chromatogr. Relat. Technol. 23, 855–872.
Teijeiro, S.A., Raviolo, M.A., Motura, M.I., Briñón, M.C., 2003. 3′-Azido-3′-deoxy-5′-*O*-isonicotinoylthymidine: a novel antiretroviral analog of zidovudine. II. Stability in aqueous media and experimental and theoretical ionization constants. Nucleosides Nucleotides Nucleic Acids 22, 1789–1803.
Teijeiro, S.A., Briñón, M.C., 2006. 3′-Azido-3′-deoxy-5′-*O*-isonicotinoylthymidine: a novel antiretroviral analog of zidovudine. III. Solubility studies. Nucleosides Nucleotides Nucleic Acids 25, 191–202.
Turk, G., Moroni, G., Pampuro, S., Briñón, M.C., Salomón, H., 2002. Antiretroviral activity and cytotoxicity of novel zidovudine (AZT) derivatives and the relation to their chemical structure. Int. J. Antimicrob. Agents 20, 282–288.
Waynforth, H.B., Flecknell, P.A., 1992. Experimental and Surgical Techniques in the Rat. Academic Press, London.
Welling, P.G., 1997. Pharmacokinetics. Processes, Mathematics, and Applications. ACS Professional Reference Book, Washington.
Wientjes, M.G., Au, J.L., 1992. Lack of pharmacokinetic interaction between intravenous 2′,3′-dideoxyinosine and 3′-azido-3′-deoxythymidine in rats. Antimicrob. Agents Chemother. 36, 665–668.